Proc. Indian Acad. Sci. (Chem. Sci.), Vol. 104, No. 5, October 1992, pp. 591–601.

Design and fabrication of an automated thermal desorption gas–solid reaction system: Oxidation of ammonia and methanol over $YBa_2Cu_3O_{7-\delta}$(123) oxide systems+

M S HEGDE*, S RAMESH and G S RAMESH

Solid State and Structural Chemistry Unit, Indian Institute of Science, Bangalore 560012, India

MS received 30 March 1992; revised 18 June 1992

Abstract. A fully automated, versatile Temperature Programmed Desorption (TDP), Temperature Programmed Reaction (TPR) and Evolved Gas Analysis (EGA) system has been designed and fabricated. The system consists of a micro-reactor which can be evacuated to 10^{-6} torr and can be heated from 30 to 750°C at a rate of 5 to 30°C per minute. The gas evolved from the reactor is analysed by a quadrupole mass spectrometer (1–300 amu). Data on each of the mass scans and the temperature at a given time are acquired by a PC/AT system to generate thermograms. The functioning of the system is exemplified by the temperature programmed desorption (TPD) of oxygen from $YBa_2Cu_{3-x}Co_xO_{7\pm\delta}$, catalytic ammonia oxidation to NO over $YBa_2Cu_3O_{7-\delta}$ and anaerobic oxidation of methanol to CO_2, CO and H_2O over $YBa_2Cu_3O_{7-\delta}$ (Y123) and $PrBa_2Cu_3O_{7-\delta}$ (Pr123) systems.

Keywords. Temperature programmed desorption; temperature programmed reaction; evolved gas analysis; ammonia oxidation; methanol oxidation; $YBa_2Cu_3O_{7-\delta}$ (123) oxides.

1. Introduction

Investigation of the gas–solid interface and the gas–solid reaction has been an active area of research in heterogeneous catalysis. Particularly, simple and mixed oxide catalysts have been successfully tested towards important applications like CO oxidation (Voorhoeve *et al* 1976), NO reduction (Sorenson *et al* 1974) and oxidative coupling of methane to higher hydrocarbons (Keller and Bhasin 1982). A general gas–solid reaction system with on-line product analysis facility could be used to test the reactivity and catalytic activity of a wide variety of solids. Further the system can also be used to study the desorption of a gaseous species from the bulk of a solid (Yue Wu *et al* 1989; Zhang *et al* 1990). In this article we describe the fabrication of a temperature programmable gas–solid reaction system which can be employed to study the desorption, dissociation kinetics, gas–solid and catalytic reactions of solids.

Since the advent of high temperature superconductivity in copper oxide systems, a large number of new oxides containing holes in oxygen have been discovered. In the recent past, a few catalytic and stoichiometric reactions have been studied with

*For correspondence

+Contribution no. 847 from Solid State and Structural Chemistry Unit

$YBa_2Cu_3O_{7-\delta}$ and related oxide systems (Hansen *et al* 1988; Mizuno *et al* 1988; Tabata 1988; Lee and Ng 1989; Halasz *et al* 1990). The utility of our experimental system is exemplified by a temperature programmed desorption study of oxygen from the $YBa_2Cu_{3-x}Co_xO_{7-\delta}$ oxides, catalytic oxidation of ammonia over $YBa_2Cu_3O_{7-\delta}$ (Y123) and anaerobic oxidation of methanol over Y123 and $PrBa_2Cu_3O_{7-\delta}$ (Pr123) oxide systems. These oxides were chosen because of the ease with which the oxygen stoichiometry can be varied (Manthiram *et al* 1987).

2. Design and fabrication

The schematic diagram of the system is shown in figure 1. The system consists of (a) a high vacuum gas handling unit with a programmable continuous flow type microreactor, (b) a mass analysis and data acquisition unit.

2.1 *High vacuum gas handling unit*

The unit consists of an all-glass high vacuum gas line designed for multiple gas handling. It can be pumped to 10^{-6} torr by a 4″ oil diffusion pump. A six millimetre dia quartz tube with an internal constriction serves as a simple continuous flow type reactor. This tube can be heated to 850°C by a programmable tubular furnace. The heating rate can be varied between 5 and 30°C per minute by a Century Systems (Bangalore) programmable temperature controller. The reactant mixture of gases is passed through fine controlled needle valves at desired flow rates varying between 10 and 100 μmol s^{-1} cm^{-2}. The flow rate is measured from the pressure difference at the source before and after the reaction. A constant flow rate is maintained during a reaction by monitoring the pressure in the gas line using a penning ionization gauge. Alternatively reactant gases premixed to a desired ratio in a single gas bulb are employed in case a mixture of gases have to be passed. The exit of the reactor is connected to the high-vacuum line as well as to an ultra high-vacuum system by means of a "T" joint. The temperature of the sample placed at the centre of the reactor is measured by a fine chromel-alumel thermocouple whose tip is kept immersed in the sample bed.

2.2 *Mass analysis and data acquisition*

The all-stainless steel ultra high vacuum system, fabricated indigenously, can be pumped to 10^{-8} to 10^{-9} torr. This system houses a VG-QXK300 quadrupole mass spectrometer with a mass range of 1–300 amu. The detector in the mass spectrometer being an electron multiplier, the time response of the spectrometer is less than a microsecond. This enables the system to differentiate and detect the masses of the gaseous products almost instantaneously. The gaseous reactants and products coming out of the microreactor are sampled through a fine leak valve for mass analysis. Mass analysis is carried out every three seconds and the data on mass peak intensities as a function of temperature is acquired employing a data acquisition system (DAS). A block diagram of the DAS is given in figure 2. The X (mass) and Y (intensity) analog signals from the mass spectrometer are buffered and fed into a multi-channel 12 bit A/D converter card which is interfaced to a personal computer. The thermocouple voltage is

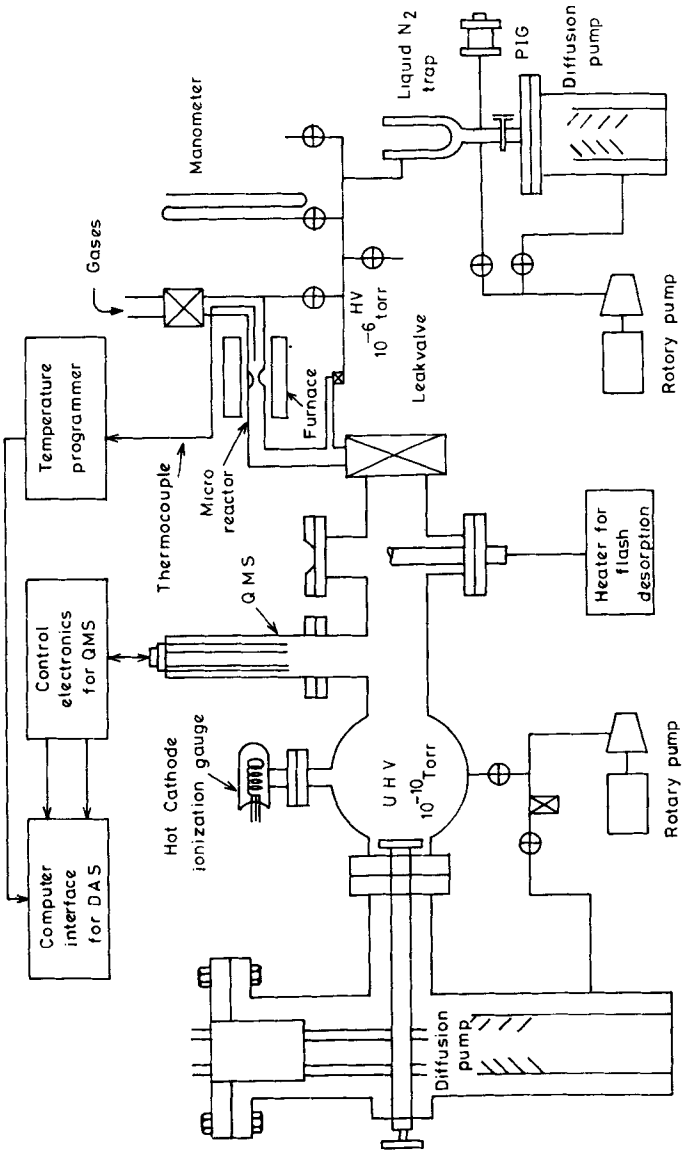

Figure 1. Schematic diagram of the gas–solid reaction system.

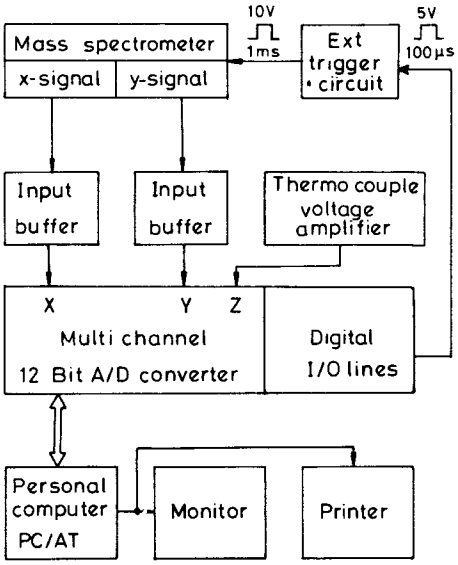

Figure 2. Block diagram showing the data acquisition system and the spectrometer interface.

Table 1. Cell parameters and oxygen content data for Y123 and Pr123.

Compound	System*	*a* (Å)	*b* (Å)	*c* (Å)	Oxygen content
$YBa_2Cu_3O_{7-\delta}$	*O*	3·815	3·891	11·649	6·95
$PrBa_2Cu_3O_{7-\delta}$	*O*	3·863	3·910	11·714	6·98
$YBa_2Cu_2CoO_{7+\delta}$	*T*	3·880	—	11·661	7·26

*O** – orthorhombic *T*– tetragonal.

also amplified and fed as the Z signal. The computer issues "start scan" signal pulses through the digital output line to an external trigger circuit to initiate each scan of the mass spectrometer. Data from X, Y and Z channels are acquired and stored in a random access file. Simultaneously, the data are plotted on a colour monitor. Finally the stored data are used to generate thermograms (mass peak intensity vs temperature).

2.3 *Preparation and characterization of materials*

The oxide series $YBa_2Cu_{3-x}Co_xO_{7\pm\delta}$, Y123 and Pr123 were prepared by heating stoichiometric mixtures of Y_2O_3, Pr_6O_{11}, BaO_2, CuO and $CoC_2O_4 \cdot 2H_2O$ at 930°C for 60 hours with three intermittent grindings, pelletized and cooled in flowing oxygen to room temperature at a rate of 1°C/min. The compounds were finely powdered and the particle sizes were determined by a Cilas–Alcatel 715E granulometer. The phase purity was checked by a JEOL JDS 8P X-ray diffractometer and the oxygen contents were estimated by iodometric titration (Harris and Hewston 1987). The cell parameters and oxygen content for Y123 and Pr123 are given in table 1. In a typical gas–solid reaction 300 mg of the oxide were placed at the centre of the reactor tube and the tip of

the thermocouple was kept immersed in the solid. Dry reactant gas/vapour was passed over the solid at a flow rate of 10 to 20 μmol s^{-1} cm^{-2} and the reactor was heated at a rate of 15°C/min over a temperature range of 30–650°C. The gaseous products were mass analysed on-line as explained earlier. The oxides were analysed after the reaction for their structures and possible formation of new solid phases (e.g. $BaCO_3$) by X-ray diffraction and infrared spectra using a Perkin–Elmer IR spectrometer.

3. Results and discussion

3.1 *TPD of oxygen from* $YBa_2Cu_{3-x}Co_xO_{7\pm\delta}$

$YBa_2Cu_3O_{7-\delta}$, a 90 K superconductor, upon heating above 300°C in N_2 atmosphere or vacuum loses oxygen and also its metallic and superconducting properties (at $\delta > 0{\cdot}6$), and transforms to a tetragonal phase (Cava *et al* 1987). Activation energy for oxygen desorption has been found to be about 28 kcal/mol (Hegde 1988). Partial substitution of Cu by Co ion in Y123 also changes the symmetry of the structure from orthorhombic to tetragonal, and, as the cobalt content increases, the superconducting transition temperature (T_c) decreases; at $x = 0{\cdot}3$ the compound becomes non-superconducting (Tarascon *et al* 1988). Since decrease in T_c has a direct correlation with the concentration of holes, TPD of oxygen was carried out to determine the effect of cobalt

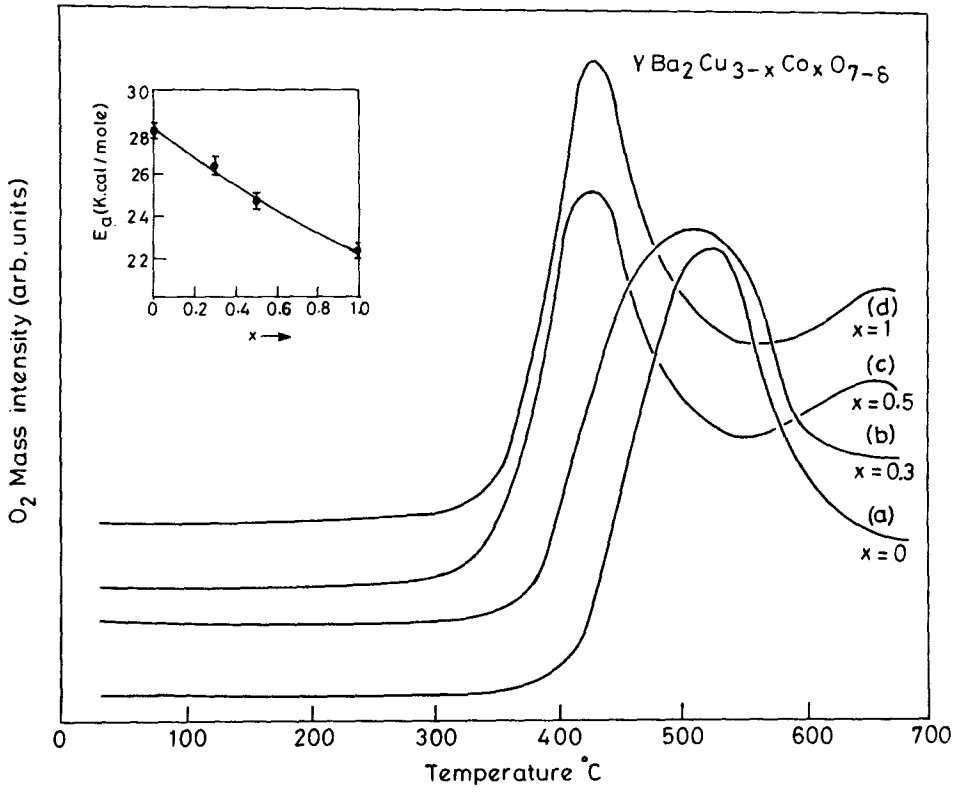

Figure 3. Temperature programmed desorption of oxygen from $YBa_2Cu_{3-x}Co_xO_{7-\delta}$ for different values of x. Inset shows E_a vs cobalt content (x).

substitution on the activation energy for oxygen desorption in the $YBa_2Cu_{3-x}Co_xO_{7-\delta}$ system of oxides. Figure 3 shows the TPD of O_2 as a function of x in $YBa_2Cu_{3-x}Co_xO_{7\pm\delta}$, for $x = 0, 0{\cdot}3, 0{\cdot}5$ and 1. The peak desorption temperature decreases from 500°C to 400°C for $x = 0$ to 1. The activation energy of oxygen desorption as obtained from the Arrhenius plots ($\ln I$ vs $1/T$) decreases with increase in cobalt content as shown in the inset of figure 3. Replacement of Cu^{2+} by Co^{3+} adds an extra electron to the system and this process contributes to the decrease in holes concentration since oxygen desorption follows the distinct steps:

$$O^{2-}(s) \xrightarrow{-e} O^{1-}(ad) \xrightarrow{-e'} O(ad) \rightarrow \tfrac{1}{2}O_2\uparrow.$$

Decrease in holes-concentration should result in the decrease in O^{1-} content and this process should increase the activation energy (E_a) of O_2 desorption. However, experimentally a decrease in E_a is observed contrary to the expectation. A careful look at the total oxygen content in $YBa_2Cu_2CoO_{7+\delta}$ shows that $\delta = 0{\cdot}25$. This is to be expected since Cu^{2+} is replaced by a Cu^{3+} ion. Assigning an oxidation state + 3 to Co under the conditions of preparation, copper is expected to be in an oxidation state of + 2·25. If this is so, the compounds should at least show metallic behaviour (Gopalakrishnan *et al* 1989). But the absence of metallicity in the oxide with $x = 1$ suggests the possible oxidation of Co^{3+} to Co^{4+} at the expense of the holes on copper. The above process could more appropriately be written as follows:

$$Cu^{3+}O^{2-} \rightleftarrows Cu^{2+}O^{1-},$$
$$Co^{4+}O^{2-} \rightleftarrows Co^{3+}O^{1-}$$

Such an equilibrium would then account for a lower E_a due to the holes on cobalt, which is a well-known observation in the case of $La_{1-x}Sr_xCoO_3$ (Zhang *et al* 1990).

3.2 *Catalytic oxidation of ammonia over* $YBa_2Cu_3O_{7-\delta}$

Figure 4a gives the reaction profiles for the anaerobic oxidation of ammonia over Y123. The products were NO, H_2O, and N_2. Onset temperature of H_2O formation from the hydrogen abstraction reaction is as low as 200°C. Desorbed oxygen also is one of the gaseous products, and it is seen that NO and H_2O are the principal products at this temperature (see figure 4a). The catalytic oxidation of ammonia was also carried out over Y123 with NH_3 and O_2 premixed in the ratio of 1:5. Figure 4b gives the reaction profiles for this catalytic oxidation. NO and H_2O were the principal products. The anaerobic oxidation of NH_3 can be attributed to the reactive chain oxygen at O(1) site resulting in the orthorhombic to tetragonal structural transition as confirmed by X-ray diffraction study. On the other hand, in the catalytic oxidation, the oxygen utilized from the O(1) site can be replenished by the molecular oxygen from the feed gas mixture and hence Y123 is not expected to undergo a structural transition which indeed is the experimental observation (Ramesh and Hegde 1992). From the above study it follows clearly that $YBa_2Cu_3O_{7-\delta}$ serves as an oxidation catalyst for the reaction:

$$2NH_3 + \tfrac{5}{2}O_2 \xrightarrow[450°C]{YBa_2Cu_3O_{7-\delta}} 2NO + 3H_2O.$$

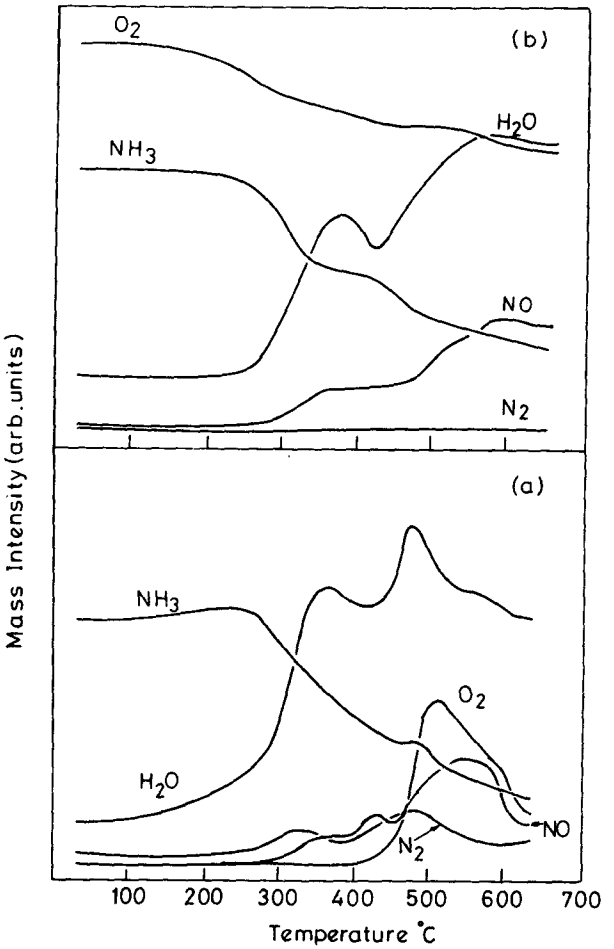

Figure 4. Temperature programmed desorption curves of (**a**) anaerobic and (**b**) aerobic oxidation of ammonia over Y123.

3.3 *Oxidation of methanol over Y123 and Pr123*

In figures 5a and b the reaction profiles of the anaerobic oxidation of methanol over Y123 and Pr123, respectively, are given. The products observed were CO_2, CO, H_2O, and H_2. On tracing the water profile it could be inferred that in the case of Y123 the reaction commences at 220°C, whereas the temperature is lowered by as much as 70°C in the case of Pr123. At 350°C CO_2 is the major product, while CO predominates at 550°C. Formation of formaldehyde at about 300°C was not observed as reported in an earlier study for a similar stoichiometric oxidation of methanol over Y123 in the presence of nitrogen carrier gas (Halasz 1989). However, they report the absence of formaldehyde at higher temperatures. The low temperature oxidation of methanol to CO_2 and water can be associated with the labile chain oxygen O(1). The oxygen associated with the holes localized in the oxygen $p\pi$ orbitals of Cu–O chain has been identified as instrumental in the anaerobic oxidation of methane (Salvador 1989).

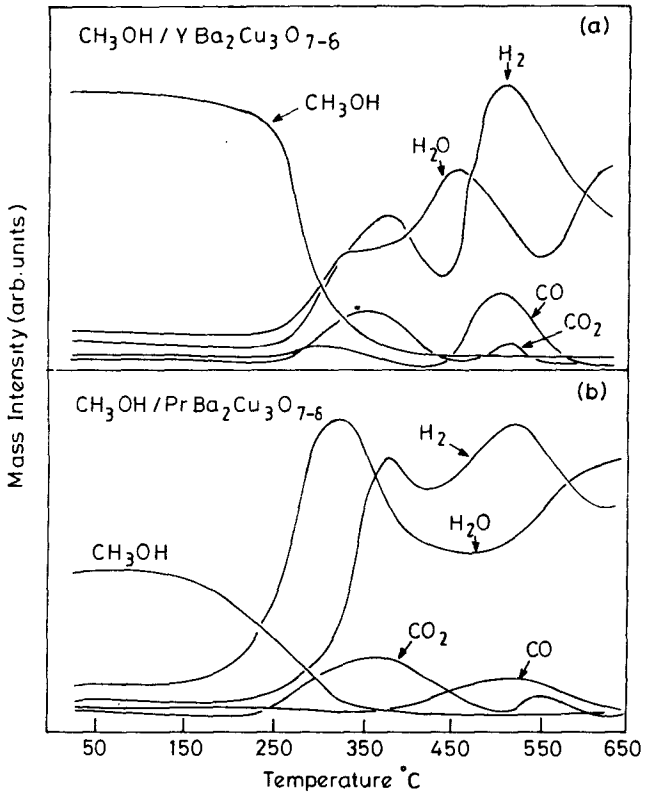

Figure 5. Temperature programmed reaction profiles for the oxidation of methanol over (**a**) Y123, and (**b**) Pr123.

At lower temperatures, the reversible variation of the oxygen stoichiometry can be made only at the O(1) sites associated with the chain oxygen (Jorgenson *et al* 1987) and any process that depletes the chain oxygen below a certain limit ($\delta > 0{\cdot}5$) should be accompanied by an orthorhombic to tetragonal structural transition (Gallaher *et al* 1987). Both these effects were indeed observed in this study. Figure 6 gives the X-ray diffractograms of the fresh and reacted Y123 and Pr123. Curves a and c depict clean structural transition from orthorhombic to tetragonal phase in the case of Y123. From the above observation it can be inferred that at lower temperatures the reaction proceeds with the consumption of the reactive chain oxygen. Once the chain oxygen is completely removed, further oxidation can proceed only with the oxygen associated with the Cu–O sheets, leading to the decomposition to basic oxides. This effect is pronounced in the case of the more reactive Pr123 as evidenced from curves b and d (figure 6). A similar mechanism for the oxidation of carbon monoxide by chain oxygen in Y123 has been reported earlier (Jiang *et al* 1989; Pickering and Thomas 1991). Taking into account the above facts, the chemical reactions occurring at the two temperature ranges have been proposed as follows. At lower temperatures ($<400°C$) the reaction taking place may be

$$CH_3OH + 2YBa_2Cu_3O_7 \rightarrow CO_2 + H_2O + H_2 + 2YBa_2Cu_3O_6.$$

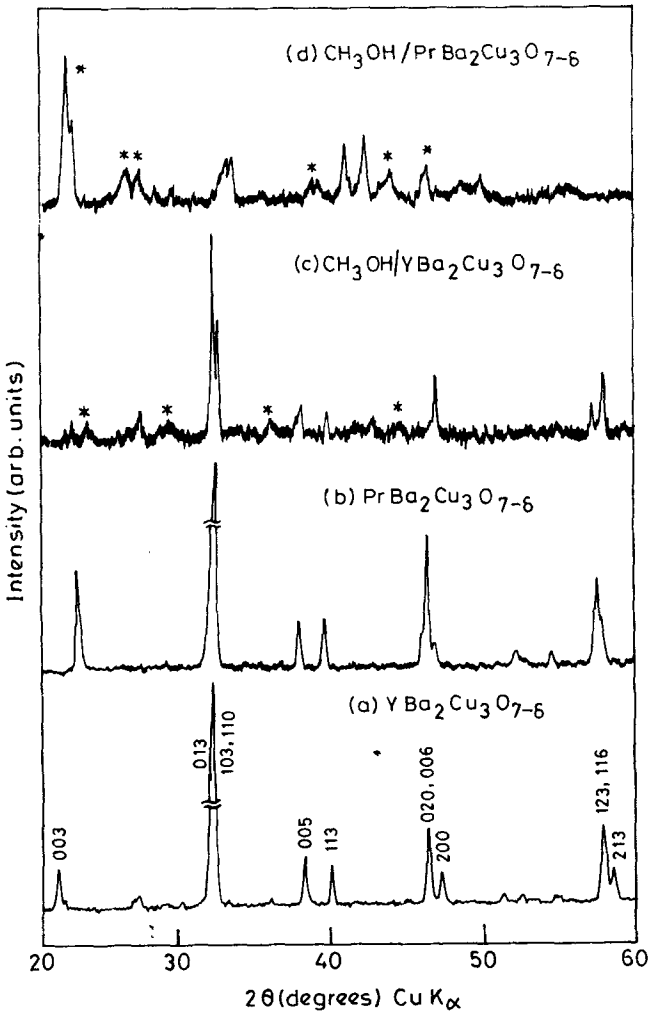

Figure 6. X-ray diffractograms of (a) Y123, (b) Pr123, (c) spent solid in the Y123/methanol reaction, and (d) spent solid in the Pr123/methanol reaction. (Asterisks denote impurity phases in the spent solids.)

At high temperature ($>450°C$) the direct oxidation of methanol to CO, H_2, H_2O predominates

$$2CH_3OH + 2YBa_2Cu_3O_6 \rightarrow 2CO + 2H_2 + 2H_2O + Y_2O_3 + 4BaO + 3Cu_2O.$$

Another important factor which influences the course and kinetics of these gas–solid reactions is the re-adsorption of carbon dioxide on the solid surface forming carbonates. Figure 7 gives the infrared spectra of the fresh and spent solids in the range of 1800 to 300 cm^{-1} as recorded by the KBr pellet method. IR spectra of Y123 is representative of its metallic nature. The bands at 1415 and 845 cm^{-1} are characteristic of the CO_3^{-2} anion and hence the formation of surface carbonates. This assignment is

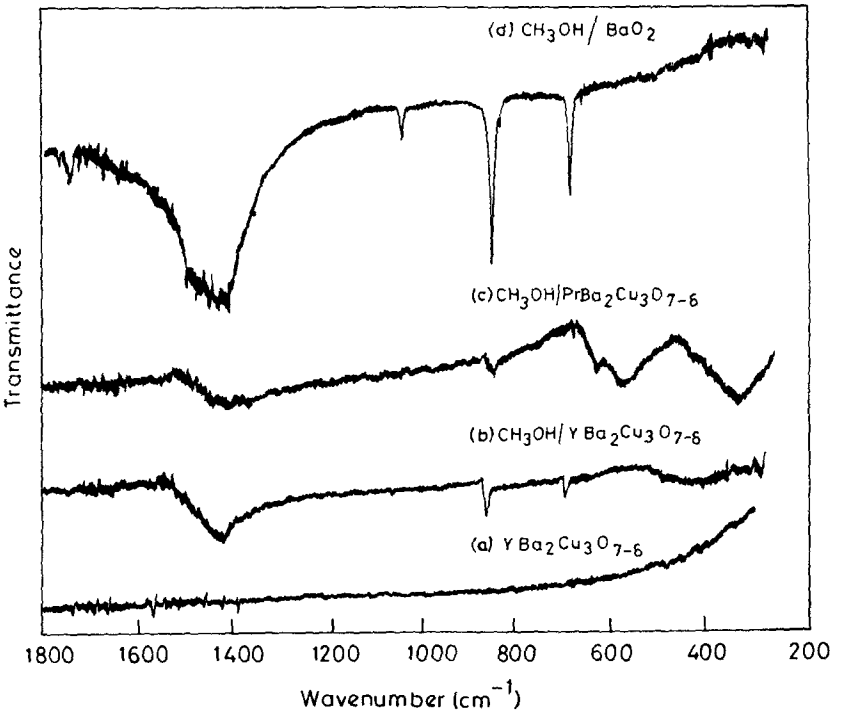

Figure 7. IR spectra of (a) Y123, (b) spent solid in the Y123/methanol reaction, (c) spent solid in the Pr123/methanol reaction and (d) spent solid in the BaO_2/methanol reaction.

further supported by the well-defined formation of barium carbonate on the anaerobic oxidation of methanol over the barium peroxide (curve d, figure 7).

4. Conclusions

(a) A versatile, gas–solid and catalytic reaction monitoring system has been fabricated and interfaced to a computer.
(b) The activation energy for oxygen desorption decreases with increase in the cobalt content in the $YBa_2Cu_{3-x}Co_xO_{7\pm\delta}$ oxide system indicating holes on both Cu and Co ions.
(c) Anaerobic oxidation of ammonia over Y123 produces N_2, NO, and H_2O whereas aerobic oxidation is NO specific.
(d) Stoichiometric oxidation of methanol by the chain oxygen in the case of the Y123 system is associated with the orthorhombic to tetragonal structural transition at low temperature.

Acknowledgements

The authors thank Prof C N R Rao for help and encouragement. One of the authors (SR) thanks the University Grants Commission for a fellowship. Financial assistance

from the Department of Science and Technology, Government of India, is gratefully acknowledged.

References

Cava R J, Batlogg B, Chen C H, Rietman E A, Zahurak S M and Werder D 1987 *Nature (London)* **329** 423
Gallagher P K, O'Bryan H M, Sunshine S A and Murphy D W 1987 *Mater. Res. Bull.* **22** 995
Gopalakrishnan J, Subramanian M A and Sleight A W 1989 *J. Solid State Chem.* **80** 156
Halasz I 1989 *Appl. catal.* **47** L17
Halasz I, Brenner A, Shelef M and Ng K Y S 1990 *J. Catal.* **126** 109
Hansen S, Otamiri C J, Jan-Olov Bovin and Andersson A 1988 *Nature (London)* **334** 14
Harris D C and Hewston T A 1987 *J. Solid State Chem.* **69** 182
Hegde M S 1988 *Mater. Res. Bull.* **23** 1171
Jiang A, Peng Y, Zhou Q, Gao P, Yuan H and Deng 1989 *J. Catal. Lett.* **3** 235
Jorgenson J D, Beno M A, Hinks D G, Soderholm L, Volin K J, Hitterman R L, Grace J D, Schuller I K, Serge C V, Zhang K and Kleefisch M S 1987 *Phys. Rev.* **B36** 3608
Keller G E and Bhasin M M 1982 *J. Catal.* **73** 9
Lee I and Ng K Y S 1989 *Catal. Lett.* **2** 403
Manthiram A, Swinnea J S, Sui Z T, Steinfink H and Goodenough J B 1987 *J. Am. Chem. Soc.* **109** 6667
Mizuno N, Yamato M, Misono M 1988 *J. Chem. Soc., Chem. Commun.* 887
Pickering I J and Thomas J M 1991 *J. Chem. Soc., Faraday Trans.* **87** 3067
Ramesh S and Hegde M S 1992 *J. Catal.* **135** 335
Salvador P 1989 *J. Phys. Chem.* **93** 8278
Sorenson S C, Wronkiewicz J A, Sis L B and Wtitz G P 1974 *Ceram. Bull.* **53** 446
Tabata K 1988 *J. Mater. Sci. Lett.* **7** 147
Tarascon J M, Barboux P, Miceli P F, Greene L H and Hull G W 1988 *Phys. Rev.* **B37** 7458
Voorhoeve R J H, Remeika J P and Trimble L E 1976 *Ann. N. Y. Acad. Sci.* **272** 3
Yue Wu, Tao Yu, Bo-Sheng Dou, Cheng-Xian Wang, Xiao-Fan Xie, Zuo-Long Yu, Shu-Rong Fan, Zhi-Rong Fan and Lian-Chi Wang 1989 *J. Catal.* **120** 88
Zhang H M, Shimizu Y, Teraoka Y, Míura N and Yamazoe N 1990 *J. Catal.* **121** 432